Sporopollenin, a natural copolymer, is robust under high hydrostatic pressure

Wren Montgomery,[a] Christian Potiszil [a], Jonathan S. Watson[a] and Mark A. Sephton[a]

[a]*Department of Earth Science and Engineering, Imperial College London, South Kensington, London SW7 2AZ*

Abstract:

Lycopodium sporopollenin, a natural copolymer, shows exceptional stability under high hydrostatic pressures (10 GPa) as determined by in situ high pressure synchrotron source FTIR spectroscopy. This stability is evaluated in terms of the component compounds of the sporopollenin: p-coumaric acid, phloretic acid, ferulic acid, and palmitic and sebacic acids, which represent the additional n-acid and n-diacid components. This high stability is attributed to interactions between these components, rather than the exceptional stability of any one molecular component. We propose a biomimetic solution for the creation of polymer materials that can withstand high pressures for a multitude of uses in aeronautics, vascular autografts, ballistics and light-weight protective materials.

Summary figure (black and white):



Introduction:

The biomimetic concept relies on natural products for providing inspiration for the development of new materials.[1] Biomimicry has recently resulted in developments across many fields of materials engineering including synthetic spider silk,[2] artificial fingerprints,[3] self-fueling motors,[4] and new platforms for tissue engineering.[5] One area of interest in materials science in which biomimicry has not yet been utilized is the identification of polymer materials that can withstand high pressures for a multitude of uses[6, 7] in aeronautics,[8] vascular autografts,[9] ballistics and light-weight protective materials.[10]

Polymers have been increasingly well-studied under pressure [11, 12] but co-polymers, combinations of more than one type of monomer, have not received equal attention. Experiments have suggested that below 20 GPa, single-component polymers such as polyethylene undergo an unusually rapid increase in stiffness and density, which slows with increased pressure. [11] The sole previous study of a co-polymer, Kel-F,[13] to high pressure revealed similar responses as observed for single-component polymer counterparts.

Sporopollenin is a naturally occurring biopolymer which forms the outer wall of spores and pollen. This natural copolymer includes compounds such as *trans*-ferulic acid ($C_{10}H_{10}O_4$), *p*-coumaric acid ($C_9H_8O_3$) and phloretic acid (3-(4-hydroxyphenyl)propanoic acid) ($C_9H_{10}O_3$), *n*-acids and di-*n*-acids.[14-16] The sporopollenin of *Lycopodium* spores play an important role in the geologic record as a potential proxy for past UV-B flux.[17, 18] Further, these natural capsules have been proposed for many different applications, including pharmaceutical delivery,[19, 20] use as microreactors,[21, 22] and heavy metal remediation.[23, 24] The responses of *Lycopodium* spores to heat and diagenesis (early post-burial modification of sedimentary materials) has been well-studied in the context of the geologic record,[15, 25, 26] but the effects of hydrostatic pressures not normally encountered in the subsurface are unprecedented.

To evaluate the effects of hydrostatic pressure as distinct from temperature (inextricably associated with pressure under geologic conditions), we used in situ synchrotron source FTIR spectroscopy to study the response of sporopollenin

capsules from *Lycopodium clavatum*, the monomers, ferulic acid, phloretic acid (3-(4-hydroxyphenyl)propanoic acid) and *p*-coumaric acid, and the representative *n*-acids palmitic and sebacic acid, to pressures of up to 10 GPa in the diamond anvil cell. Sporopollenin was found to be far more resistant to pressure than any of its monomeric components, and more stable than Kel-F, the only co-polymer for which there is high-pressure data available.[13]

Sporopollenin from *Lycopodium clavatum* were subjected to hydrostatic pressures of up to 10 GPa in a diamond anvil cell (DAC) as shown in Figure 1 while using in situ high pressure synchrotron source FTIR spectroscopy to monitor chemical bond formation and destruction. Solvent extracted *Lycopodium* spores were loaded individually. Through trial and error, we determined that three overlapping spores (approx. 50-100 micron diameter in total) gave the best signal (Figure 1a).

Experimental Section

Samples were loaded by hand into a membrane-driven diamond anvil cell containing Type II diamonds with culets of 0.5 mm diameter. A pre-indented gasket of 0.15 mm thickness containing a sample chamber hole of 0.25 mm diameter was placed between the gaskets. A cesium iodide (CsI) window was prepared before samples were loaded, along with a small (<0.05 mm diameter) ruby sphere (Figure 1b). Pressures were monitored throughout the experiment using the ruby fluorescence technique.[27] The fluorescence signal was measured using a compact fixed-grating spectrometer unit (Ocean Optics HR4000) that included a 800 line/mm grating read out by a linear CCD chip that had 4096 pixels. Error in the pressure calculation owing to the precision of the spectrometer unit was calculated to be less than 0.01 GPa; the uncertainty of the pressure in the diamond anvil cell because of nonhydrostatic conditions was estimated to be ±0.1 GPa. Further details of the system geometry and synchrotron facilities can be found in previous works.[28, 29]

FTIR spectra were collected at approximately 0.5 GPa increments from the initial pressurization up to 5 GPa, and approximately 1 GPa increments up to >10 GPa (not all spectra are presented in the paper).

Transmission FTIR micro-spectrometry was performed using synchrotron source light at the SMIS beamline at SOLEIL Synchrotron (France). This beamline hosts a custom-made horizontal infrared microscope for large volume samples, which has two Schwarzchild objectives (47 mm working distance, NA 0.5) which produces a 22 micron (full width at half maximum) IR spot. To minimize the effects of non-hydrostaticity in the sample chamber, spectra were consistently collected at the same point relative to the background spectrum point and the ruby. The system spectrometer is a Nexus 6700[28] in conjunction with a liquid N_2-cooled MCT/A detector. Resolution was 4 cm^{-1} and the number of co-added scans was 25.

Background spectra were collected in a "blank" area of the sample chamber containing only the CsI window. A background was collected for every pressure and temperature combination measured prior to measurement of the sample, and the sample spectra were (re)processed using the appropriate files. These spectra were analyzed by removing the background signal and the resulting peaks were fitted as standard Gaussians using fityk[30]. Spectra from the wavenumber region 2500-4000 cm^{-1} were "defringed" using a custom program. The fringing is the result of internal reflections in the experimental setup (between the inside and outside faces of the diamond) and disproportionately affects this region.

Results and Discussion:

Once the FTIR spectra of *Lycopodium* sporopollenin were collected and processed, peak assignments were made with the aid of previously published work.[25] Known peaks are: νC=C (1517, 1632 cm^{-1}), νC=O (1704 cm^{-1}), $\nu_{sym}CH_n$ (2860 cm^{-1}), $\nu_{asym}CH_n$ (2936 cm^{-1}), and νOH (3394 cm^{-1}). In agreement with previously published work, the symbol "ν" denotes stretching vibrations and "β" will be used to denote in-plane deformations.[31-33] Peak assignments are summarized in Supplementary Table 1.

Figure 2 illustrates the stability of sporopollenin at pressures up to 10 GPa. The largest change is the decrease in relative intensity of the C-H vibrations at 2860 and 2936 cm^{-1} relative to the OH band, which indicates constrained geometry with decreasing intermolecular distances. There is very little variation in relative peak

height within the spectra. The OH vibration is asymmetric with a maximum peak height at approximately 3300 cm^{-1}. This band shows a shift towards lower wavenumbers and peak broadening with increasing pressure, which is typical for hydrogen bonding under compression. The absorption intensity on the low frequency side increases with high pressure, another indication of hydrogen bonding under pressure. Due to the broadness of the νOH peak, it was modelled as two Gaussian peaks initially centered at 3310 and 3496 cm^{-1}; this model gives a quantitative representation of the peak shape, and should not be interpreted as specific vibrational bands. These were found to change at rates of -2.2 and -0.8 cm^{-1}/GPa respectively (Figure 5a).

While the exact composition of sporopollenin is still to be determined, *p*-coumaric acid, phloretic acid and ferulic acid are primary components.[14-16] After discovering the unexpected resistance of *Lycopodium* spore exines to high pressures, we undertook an examination of these components, alongside palmitic and sebacic acids, which represent the additional *n*-acid and *n*-diacid components, to see if *Lycopodium* spore stability was due to a single component. Using the same experimental technique as above, single crystals approximately 10 x 50 x 50 microns of each sample were selected directly from the bottle (pure samples purchased from Sigma-Aldrich) for crystallinity and size and loaded into the DAC.

Peak assignments have been previously made for *trans*-ferulic acid:[31] of interest to this work are νC=C (1512, 1601 cm^{-1}), νC=O (1691 cm^{-1}), νCO (1202 cm^{-1}), $\nu_{sym}CH_n$ (2943 cm^{-1}), $\nu_{asym}CH_n$ (2963 cm^{-1}), and νOH (3079 (COOH) and 3440 cm^{-1}). At the lower wavenumbers, the most significant change is to the νC=O frequency, which is suppressed with increasing pressure. A peak at 1379 cm^{-1} assigned to CH_3 symmetric deformation vanishes at pressures above 5.0 GPa. (Figure 3a)

Peak assignments have been previously made for *p*-coumaric acid:[32] of interest to this work are νC=C (1516, 1601 cm^{-1}), νC=O (1682 cm^{-1}), νCO (1283 cm^{-1}), νCH_n (2963, 3026 , 3073 cm^{-1}), and νOH (3381 cm^{-1}). In the lower wavenumber range, *p*-coumaric acid undergoes only small, subtle changes with pressure involving the disappearance of peaks, specifically βOH_{ar} at 1258 cm^{-1}, $\beta CH_{C=C}$ at 1425 cm^{-1} (in-

plane deformations) and $\nu CC_{C=C}$ at 1624 cm^{-1} (stretching vibration) (Figure 3b). This suggests that the C=C bond between the accessible aromatic part of the molecule and the carboxyl group is becoming more constrained with the decreasing volume associated with higher pressures.

Peak assignments have not been previously made for phloretic acid. The following assignments have been made on the basis of comparison with similar molecules: $\nu C=O$ (1695 cm^{-1}), νCO (1293 cm^{-1}) and νOH (3373 cm^{-1}). In the lower wavenumber range, phloretic acid varies only slightly, the major changes being the disappearance of the $\beta OHar$ peak at 1257 cm^{-1} and the νCO peak splitting into two (Figure 3c).

Peak assignments have been made previously for palmitic acid.[34] Of interest to this work are $\nu C=O$ (1714 cm^{-1}), νCO (1275 cm^{-1}) and νOH (broad peak at 3000 cm^{-1}). In the lower wavenumber range, (Figure 3d) the most substantial changes with pressure involve the methyl and methylene vibrations present as small peaks between 1250 and 1500 cm^{-1}, which change in relative intensity with increasing pressure. The βOH peaks at 1312 and 1475 cm^{-1} show only very slight changes with increasing pressure while the C=O band moves to lower wavenumbers, suggesting that any intermolecular hydrogen bonding present is related to the presence of dimers, consistent with ambient temperature x-ray diffraction data.[35]

Finally, peak assignments have previously been made for sebacic acid.[36] Much as with palmitic acid, the bands of interest are $\nu C=O$ (1684 cm^{-1}), νCO (1297 cm^{-1}) and νOH (~3400 cm^{-1}). The small peaks associated with methyl and methylene units between 1150 and 1500 cm^{-1} decline in intensity with increasing pressure, while βOH peaks at 1285 and 1425 cm^{-1} gain intensity and shift to higher wavenumbers (Figure 3e), consistent with the formation of long chains of intermolecular O-H…O bonds in a phase transition from the dimers observed at ambient pressure using x-ray diffraction[37], as has been previously observed in formic acid[38].

In the higher wavenumber range (Figure 4a), transferulic acid shows the characteristic shift of the OH vibration to lower wavenumbers with increasing pressure at a rate of -

28.6 cm^{-1}/GPa (Figure 5b), and typically subdued CH stretching vibrations at high pressures, consistent with the geometric hindering of deformations of this group observed at lower wavenumbers. Also in the higher wavenumber range (Figure 4b), *p*-coumaric acid does not show the same shift of the OH band to lower wavenumbers as *trans*-ferulic acid, decreasing at a rate of -17.0 cm^{-1}/GPa (Figure 5c). A new peak appears at 3381 cm^{-1} at 5.0 GPa. This new peak redshifts at a rate of -7.5 cm^{-1}/GPa. (Figure 5c) Appearance of new peaks in this region can indicate the formation of new hydrogen bonds[39]. In the same wavenumber range (Figure 4c), phloretic acid demonstrates the same shift of the OH band to lower wave numbers, at a rate of -23.3 cm^{-1}/GPa, similar to that observed for *trans*-ferulic acid (Figure 5d). However, phloretic acid shows greater peak broadening than transferulic acid.

Finally, in this wavenumber range, palmitic and sebacic acid have prominent clusters of peaks in the 2800-3000 cm^{-1} region, which are due to the antisymmetric and symmetric stretching vibrations of methyl and methylene groups. Sebacic acid shows the rapid shift of the OH band to lower wavenumbers with pressure associated with pressure-induced crystallization and the formation and symmetrisation of long chains of intermolecular O-H…O bonds in carboxylic acids.[38, 40] No such shift is present in palmitic acid, again suggesting that intermolecular hydrogen bonding in this material remains limited to dimer formation.

The rate of decrease of the νOH band can be interpreted as a proxy for the strength of the bond,[41, 42] suggesting that all of the constituent components of the sporopollenin undergo greater changes under pressure than the natural material. Of those studied, only p-coumaric acid and sebacic acid show signs of new hydrogen bonding within pure samples. This suggests that interaction between the components is the stabilizing force within sporopollenin.

Conclusions:

The extreme pressure resistance of sporopollenin makes it suitable for uses requiring chemical, thermal and pressure stability. *Lycopodium* spores are unexpectedly minimally affected by pressures up to 10 GPa, in contrast to its constituent monomers, *p*-coumaric, *trans*-ferulic, palmitic and sebacic acid. *p*-Coumaric acid in isolation

shows indications of symmetric hydrogen-bonded network formation, whereas *trans*-ferulic acid and phloretic acid do not. It is possible that network formation is hindered in *trans*-ferulic acid by the presence of the methoxy group. However, phloretic acid and *p*-coumaric acid are very similar molecules, the only difference being that the latter contains a carbon-carbon double bond in its acid side chain. It is plausible that the presence of the double bond in *p*-coumaric acid promotes hydrogen bonding.

The carboxylic acid monomers show a different pattern: intermolecular hydrogen bonding is indicated in sebacic acid, the dicarboxylic acid, but not palmitic acid, possibly due to the shorter chain length and increased number of carboxyls available for bond formation in sebacic acid. When combined to make the *Lycopodium* spore exine, these five molecules combine to form an extremely stable macromolecule, perhaps owing to coupling of the hydrogen-network forming capabilities of *p*-coumaric acid and sebacic acid and the pressure resistance of *trans*-ferulic, phloretic acid and palmitic acid. This extreme resistance to pressure suggests that *Lycopodium* spores may have even broader applications than previously imagined.

Acknowledgements

We acknowledge SOLEIL synchrotron for provision of synchrotron radiation facilities (Proposal ID "20140430" and "20141394") and we thank Dr. Ferenc Borondics and Dr. P. Dumas for assistance in using beamline SMIS and Dr. J.-P. Itie for access to the high-pressure facilities of beamline PSICHÉ. The research leading to these results has received funding from the European Community's Seventh Framework Programme (FP7/2007–2013) under grant agreement No. 312284. We also acknowledge support from STFC, grant number ST/K000551/1.

Keywords: high pressure, copolymerization, biomimicry, FT-IR, hydrogen bonding

References

[1] P. Fratzl, *Interface* **2007**, *4*, 637.
[2] A. Heidebrecht, L. Eisoldt, J. Diehl, A. Schmidt, M. Geffers, G. Lang, T. Scheibel, *Adv. Mater.* **2015**, *27*, 2189.
[3] H. J. Bae, S. Bae, C. Park, S. Han, J. Kim, L. N. Kim, K. Kim, S.-H. Song, W. Park, S. Kwon, *Adv. Mater.* **2015**, *27*, 2083.

[4] J. Zhang, Y. Yao, L. Sheng, J. Liu, *Adv. Mater.* **2015**, *27*, 2648.
[5] J. G. Torres-Rendon, T. Femmer, L. De Laporte, T. Tigges, K. Rahimi, F. Gremse, S. Zafarnia, W. Lederle, S. Ifuku, M. Wessling, J. G. Hardy, A. Walther, *Adv. Mater.* **2015**, *27*, 2989.
[6] A. J. Liu, G. S. Grest, M. C. Marchetti, G. M. Grason, M. O. Robbins, G. H. Fredrickson, M. Rubinstein, M. Olvera de la Cruz, *Soft Matter* **2015**, *11*, 2326.
[7] A. L. Kovarskii, Ed. *High Pressure Chemistry and Physics of Polymers*, CRC, Boca Raton **1994**.
[8] H.-X. Peng, in *Multifunctional Polymer Nanocomposites*, (Eds: J. Leng, K.-T. Lau), Taylor & Francisc Group, **2011**, 337.
[9] Y. Ichihara, T. Shinoka, G. Matsumura, Y. Ikada, K. Yamazaki, *Interactive CardioVascular and Thoracic Surgery* **2015**, *20*, 768.
[10] R. G. S. Barsoum, "Elastomeric Polymers for Shockwave Mitigation and Extreme Londing Conditions", presented at 2013 Annual Conference on Experimental and Applied Mechanics, Costa Mesa, CA, USA, **2012**.
[11] L. Fontana, M. Santoro, R. Bini, D. Q. Vinh, S. Scandolo, *J. Chem. Phys.* **2010**, *133*, 204502.
[12] W. Li, D. Duan, X. Huang, X. Jin, X. Yang, S. Li, S. Jiang, Y. Huang, F. Li, Q. Cui, Q. Zhou, B. Liu, T. Cui, *J. Phys. Chem. C* **2014**, *118*, 12420.
[13] A. S. Benjamin, M. Ahart, S. A. Gramsch, L. L. Stevens, E. B. Orler, D. M. Dattelbaum, R. J. Hemley, *J. Chem. Phys.* **2012**, *137*, 014514.
[14] P. Blokker, D. Yeloff, P. Boelen, R. A. Broekman, J. Rozema, *Anal. Chem.* **2005**, *77*, 6026.
[15] J. S. Watson, W. T. Fraser, M. A. Sephton, *J. Anal. Appl. Pyrolysis* **2012**, *95*, 138.
[16] J. S. Watson, M. A. Sephton, S. V. Sephton, S. Self, W. T. Fraser, B. H. Lomax, I. Gilmour, C. H. Wellman, D. J. Beerling, *Photochemical & Photobiological Sciences* **2007**, *6*, 689.
[17] B. H. Lomax, W. T. Fraser, G. Harrington, S. Blackmore, M. A. Sephton, N. B. W. Harris, *Earth. Planet. Sci. Lett.* **2012**, 353-354.
[18] B. H. Lomax, W. T. Fraser, M. A. Sephton, T. V. Callaghan, S. Self, M. Harfoot, J. A. Pyle, C. H. Wellman, D. J. Beerling, *Nat. Geosci.* **2008**, *1*, 592.
[19] S. U. Atwe, Y. Ma, H. S. Gill, J. *Controlled Release* **2014**, *194*, 45.
[20] A. Diego-Taboada, L. Maillet, J. H. Banoub, M. Lorch, A. S. Rigby, A. N. Boa, S. L. Atkin, G. Mackenzie, *J. Mater. Chem. B* **2013**, *1*, 707.
[21] S. A. Hamad, A. F. K. Dyab, S. D. Stoyanov, V. N. Paunov, *J. Mater. Chem.* **2011**, *21*, 18018.
[22] V. N. Paunov, G. Mackenzie, S. D. Stoyanov, *J. Mater. Chem.* **2007**, *17*, 609.
[23] A. Çáimen, A. Bilgiç, A. N. Kursunlu, İ. H. Gübbük, H. İ. Uçan, *Desalination and Water Treatment* **2013**, *52*, 4837.
[24] İ. Sargın, G. Arslan, *Int. J. Biol. Macromol.* **2015**, *75*, 230.
[25] W. T. Fraser, J. S. Watson, M. A. Sephton, B. H. Lomax, G. Harrington, W. D. Gosling, S. Self, *Review of Palaeobotany and Palynology* **2014**, *201*, 41.
[26] P. A. Schenk, J. W. d. Leeuw, G. v. Graas, J. Haverkamp, M. Bouman, in *Organic Maturation Studies and Fossil Fuel Exporation*, (Ed: J. Brooks), Academic Press, London **1981**, 225.
[27] H. K. Mao, J. Xu, P. M. Bell, *Journal of Geophysical Research: Solid Earth* **1986**, *91*, 4673.
[28] P. Dumas, F. Polack, B. Lagarde, O. Chubar, J. L. Giorgetta, S. Lefrançois, *Infrared Phys. Technol.* **2006**, *49*, 8.

[29] E. Jennings, W. Montgomery, P. Lerch, *J. Phys. Chem. B* **2010**, *114*, 15753.
[30] M. Wojdyr, *J. Appl. Crystallogr.* **2010**, *43*, 1126.
[31] S. Sebastian, N. Sundaraganesan, S. Manoharan, *Spectrochim. Acta, Part A* **2009**, *74*, 312.
[32] R. Swislocka, M. Kowczyk-Sadowy, M. Kalinowska, W. Lewandowski, *Spectroscopy* **2012**, 27.
[33] G. Varsányi, *Assignments for vibrational spectre of seven hundred benzene derivatives*, Adam Hilger, London **1974**.
[34] I. R. Hill, I. W. Levin, *J. Chem. Phys.* **1979**, *70*, 842.
[35] S. Bhattacharya, V. G. Saraswatula, B. K. Saha, *Crystal Growth & Design* **2013**, *13*, 3651.
[36] C. E. Hathaway, in Physics, Vol. PhD, University of Oklahoma, Norman, Oklahoma **1965**, 190.
[37] E. Moreno, R. Cordobilla, T. Calvet, F. J. Lahoz, A. I. Balana, *Acta Crystallogr. Sect. C: Cryst. Struct. Commun.* **2006**, *62*, o129.
[38] A. F. Goncharov, R. F. Manaa, J. M. Zaug, R. H. Gee, L. E. Fried, W. Montgomery, *Phys. Rev. Lett.* **2005**, 94.
[39] C. Murli, N. Lu, Z. Dong, Y. Song, *J. Phys. Chem. B* **2012**, *116*, 12574.
[40] W. Montgomery, J. M. Zaug, W. M. Howard, A. F. Goncharov, J. C. Crowhurst, R. Jeanloz, *J. Phys. Chem. B* **2005**, *109*, 19443.
[41] H. Bhatt, A. K. Mishra, C. Murli, A. K. Verma, N. Garg, M. N. Deo, S. M. Sharma, *Phys. Chem. Chem. Phys.* **2016**, *18*, 8065.
[42] G. Zundel, *J. Mol. Struct.* **2000**, *552*, 81.

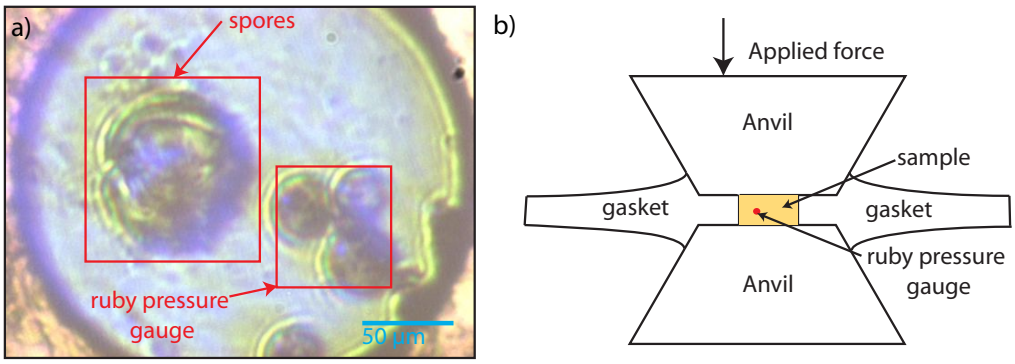


Figure captions:

Figure 1. a) microphotograph of *Lycopodium* sample loaded into the diamond anvil cell. b) schematic (not to scale) of the diamond anvil cell assembly. (Color online.)

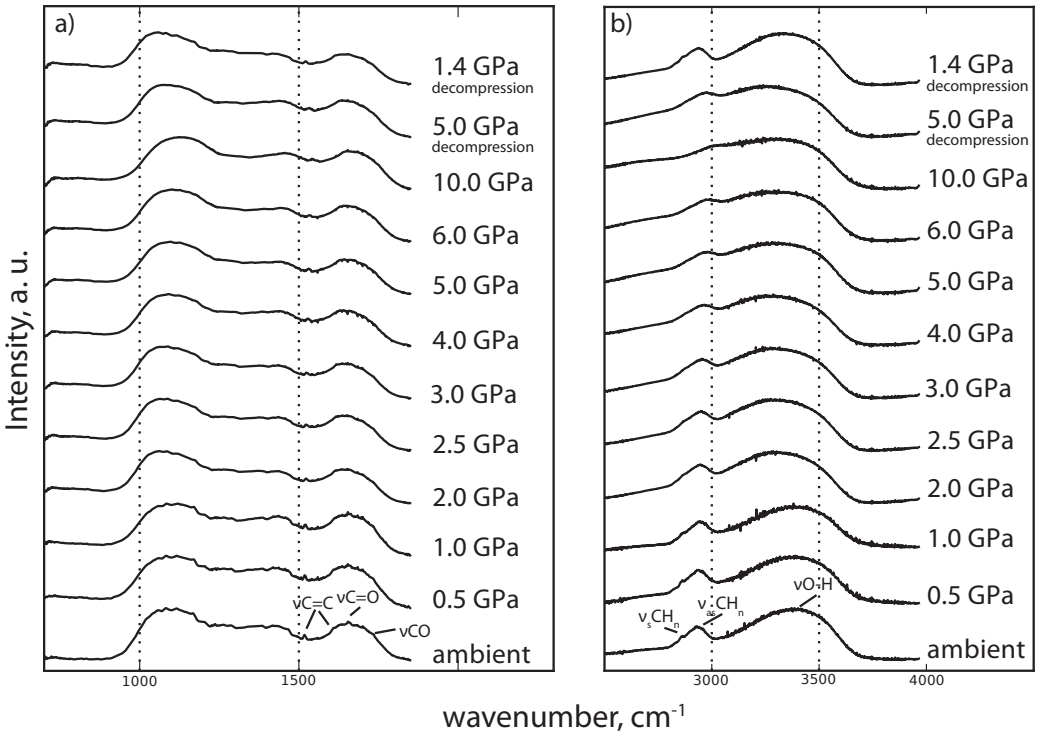


Figure 2. FTIR spectra of sporopollenin from *Lycopodium clavatum* from ambient pressure to 10.0 GPa. a) shows the wavenumber range 700-1800 cm^{-1}, and b) shows the hydrogen-bonding frequency range, 2500-4000 cm^{-1}. A shift in the peak center and relative intensity is observed above 1.0 GPa. All spectra are normalized to the local maximum over the range 700-4000 cm^{-1}.

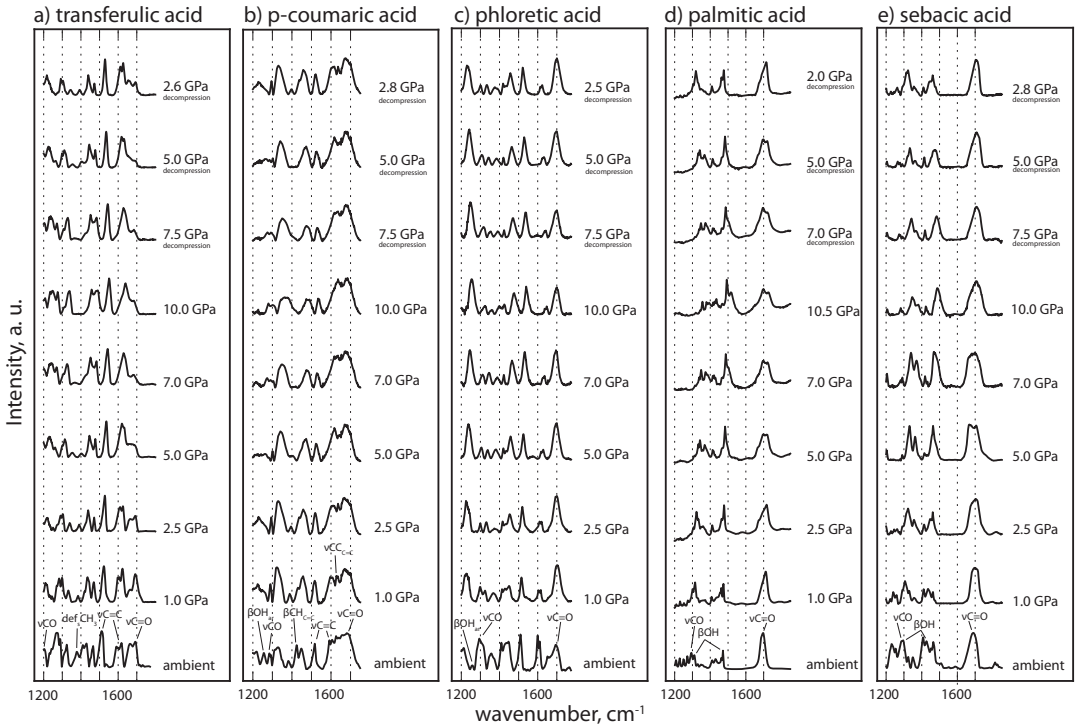


Figure 3. FTIR spectra at pressures up to 10 GPa in the fingerprint region of 1200-1700 cm^{-1} of: a) *trans*-ferulic acid, b) *p*-coumaric acid, c) phloretic acid (3-(4-hydroxyphenyl)propanoic acid), d) palmitic acid and e) sebacic acid.

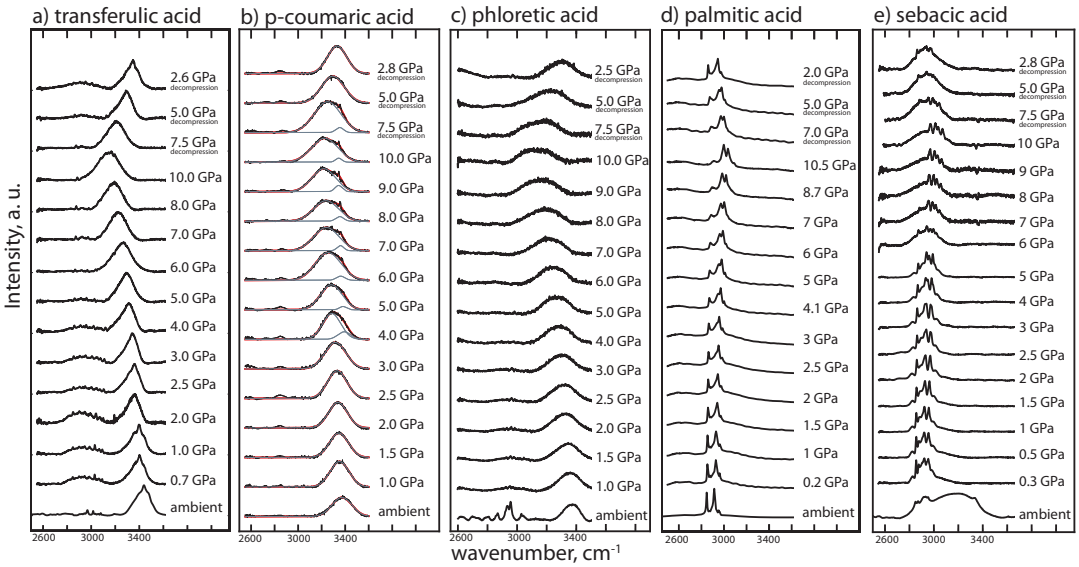


Figure 4. FTIR spectra of a) *trans*-ferulic acid, b) *p*-coumaric acid c) phloretic acid (3-(4-hydroxyphenyl)propanoic acid), d) palmitic acid and e) sebacic acid in the hydrogen bonding region (2600-3500 cm^{-1}). In a) and c) the typical pressure-induced red shift to a lower wavenumber is apparent. Note also the suppression of the CH vibrational bands centered around 2900 cm^{-1} at pressures above 5.0 GPa. In b), the

redshift is much smaller, and the appearance of a small distinct peak at 3381 cm^{-1} at pressures above 5 GPa is associated with the formation of intermolecular O-H…O bonds. Grey curves are the result of fitting to a two-curve model. Palmitic acid, (d), is little affected by pressure, and sebacic acid (e) shows the rapid change associated with crystallization between spectra collected at ambient and 0.3 GPa pressures.

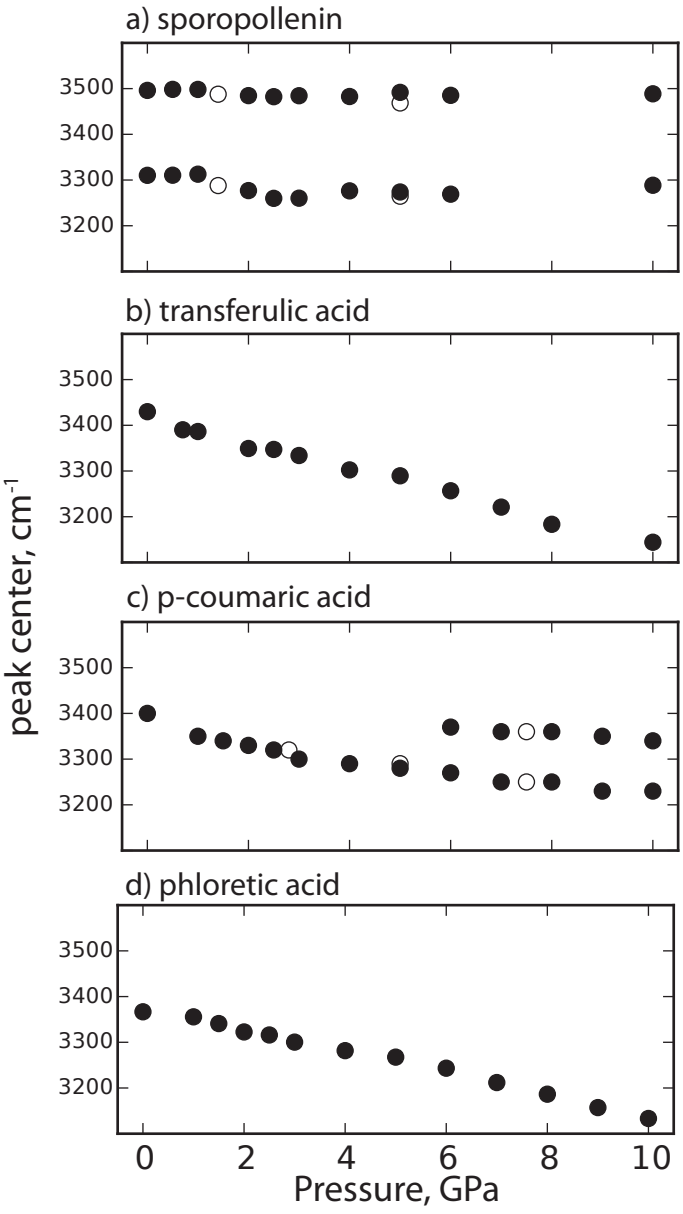


Figure 5. a) Using a two-peak model, the νOH band of sporopollenin is calculated to downshift at rates of -0.8 and -2.2 cm^{-1}/GPa. b) The νOH band of transferulic acid, modelled as a single peak, redshifts at -28.6 cm^{-1}/GPa. c) The νOH band of p-

coumaric acid evolves a second peak at 5.0 GPa. The main band shifts by 17.0 cm^{-1}/GPa, while the new band moves at -7.5 cm^{-1}/GPa. d) The νOH band of phloretic acid, fit to a single Gaussian, changes at a rate of -23.3 cm^{-1}/GPa.

Table of Contents text and graphic

Lycopodium sporopollenin, a natural copolymer, shows exceptional stability under high hydrostatic pressures (10 GPa) as determined by in situ high pressure synchrotron source FTIR spectroscopy. This stability is evaluated in terms of the component compounds of the sporopollenin and attributed to interactions between these components, rather than the exceptional stability of any one molecular component.

Figure :

